A way to determine groundwater contributions to large river systems: The Elbe River during drought conditions

Julia Zill [a,*], Christian Siebert [a,*], Tino Rödiger [a], Axel Schmidt [b], Benjamin S. Gilfedder [c], Sven Frei [d], Michael Schubert [a], Markus Weitere [e], Ulf Mallast [f]

[a] *Dept. Catchment Hydrology, Helmholtz Centre for Environmental Research (UFZ), Halle (Saale) 06120, Germany*
[b] *Ref. G4 Radiology and Water Monitoring, Federal Institute of Hydrology (BfG), Koblenz 56068, Germany*
[c] *Limnological Research Station, Hydrology, Univ. of Bayreuth, Bayreuth 95447, Germany*
[d] *Wageningen University Research Centre, Department of Environmental Science, Aquatic Ecology and Water Quality Management Group, P.O. Box 47, 6700 AA Wageningen, the Netherlands*
[e] *Dept. River Ecology, Helmholtz Centre for Environmental Research (UFZ), Magdeburg 39114, Germany*
[f] *Dept. Monitoring, and Exploration Technologies, Helmholtz Centre for Environmental Research (UFZ), Leipzig 04318, Germany*

ARTICLE INFO

ABSTRACT

Study region: Our study region extends over 450 stream km of the German part of the Elbe River, an ecologically and economically important first order river, between Schöna and Wittenberge.
Study focus: Diffuse groundwater born nutrients are major contributors to increased algae growth in rivers, leading to eutrophication with serious consequences for water quality and ecosystem health. Therefore, knowledge of the spatial and temporal dynamics of diffuse groundwater discharge are required since groundwater often remains as a 'black box' for the identification of nutrient sources by managers. The multi-method approach, based on the inverse geochemical and tritium modelling, a flux balance, a darcy approach and hydraulic gradients, showed complex spatiotemporal dynamics along the studied reach of the Elbe River. Groundwater inflow was variable but occurred along the entire river. Areas of high groundwater fluxes were located in the upstream mountainous catchment areas and decreasing downstream.
New hydrological insights for the region: The multi-method approach provides a blueprint for the assessment of other large river systems. No single method was able to create conclusive results and most other approaches are only applicable in smaller stream systems. First time an estimation of groundwater flux rates, that can be used to quantify matter inputs, was made. In addition, we showed a way to detect and assess the impact of drainage channels in a heterogenous river system.

1. Introduction

Hydrological connectivity between groundwater and surface water bodies such as rivers, lakes and estuaries is vital for maintaining the ecological integrity of these systems. Groundwater discharge to rivers and streams often has a significant impact on surface water quality (Brunke and Gonser, 1997; Ibáñez and Peñuelas, 2019; Tong et al., 2015). Especially in agriculturally dominated regions, such as Central Europe, groundwater inflow is a potential source of contaminants such as pesticides and nutrients (C, N, P) in fluvial

---

ecosystems (Brookfield et al., 2021; Donohue et al., 2005; Sharpley et al., 1994; UBA, 2020). In particular, eutrophication is the result of excess of nutrient inputs into rivers, lakes and estuaries (Bachmann, 1980; Dodds, 2006; Howarth and Marino, 2006; Kamjunke et al., 2022; Lewandowski et al., 2015; Santos et al., 2021), and has been shown to negatively affect ecosystem stability and biodiversity (Dodds et al., 2009; Donald et al., 2013; Mallin et al., 2006).

Reliable localisation and quantification of groundwater inflow and its potential contaminant loads are fundamental to the development of effective management strategies with the potential to mitigate or even prevent negative consequences for fluvial ecosystems. It enables the quantification of water budgets by elucidating the exchange of water between aquifers and surface water bodies. This knowledge is fundamental for sustainable water resource management, ensuring a reliable supply of water for various sectors such as agriculture, industry, and domestic use (Gleeson et al., 2012). A comprehensive understanding of these interactions is essential for planning the safety of water abstraction from large rivers, as it helps prevent the over-extraction of water resources (Richter et al., 2012). In riverine areas insights into groundwater-surface water interactions are critical for effective flood management and flood prediction. This information aids in developing strategies to mitigate flood risks, safeguarding both human communities and natural environments (Merz and Blöschl, 2003). Such knowledge also improves the conceptual understanding of river-aquifer interactions allowing a better characterisation. Additionally, existing numerical models which suffer from a lack of parameterization due to sparse existing data could specify their boundary conditions and set ups to simulate the connected groundwater system (Fleckenstein et al., 2010; Hillel et al., 2019; Rhodes et al., 2017).

In particular, large river systems need to be studied to provide the basis for national strategies for holistic management of coupled aquatic systems for different purposes such as drought management or water quality (Neal et al., 2000). Since the establishment of the Water Framework Directive (EU WFD, 2000), water quality has been monitored in large river basins across Europe e.g. Loire and Seine (Even et al., 2007; Larroudé, . et al., 2013), Danube and Rhine (Chapman et al., 2016; Mostert, 2008), Thames (Bowes et al., 2018), Ebro (Bouza-Deaño et al., 2008), Po (Panepinto et al., 2015) or the Volga (Schletterer et al., 2019). However, in these large rivers, sufficient causal research and analyses of deteriorating inflows were restricted to short river reaches (Hutchins et al., 2018; Kalugin, 2019; Lalot et al., 2015; Lasagna et al., 2016; Rhodes et al., 2017).

Commonly used methods to characterise groundwater discharge to surface water bodies include physical methods like heat as a tracer (Close et al., 2016; Malard et al., 2001), electrical conductivity (Oehler et al., 2018; Vogt et al., 2010), or hydraulic parameters (Botting, 2010; Cheng et al., 2010; Larned et al., 2008; Larned et al., 2015; Vincent, 2005). Alternatively, chemical methods can also be used to quantify groundwater inflow either through continuous tracer mapping, such as ^{222}Rn (Moore, 1997; Ortega et al., 2015; Schmidt et al., 2009; Schubert et al., 2020; Yu et al., 2013), or discrete samples of δ^2H, δ^{18}O, ^{36}Cl, ^{3}H, ^{4}He, CFCs, SF$_6$ (Botting, 2010; Burbery and Ritson, 2010; Cantafio and Ryan, 2014; Cook et al., 2003; Cook, 2013; Gardner, 2011; McCallum et al., 2012; Schmidt et al., 2010; Wang et al., 2008). Although groundwater inflow occurs at all scales (Bertrand et al., 2014; Puckett et al., 2008), most of these approaches have historically been preferentially applied to smaller stream systems (Coluccio and Morgan, 2019; Cook, 2013; Kalbus et al., 2006; Rosenberry and LaBaugh, 2008; Unland et al., 2013;), while they fail or are impracticable in large 1st or 2nd order rivers. At the scale of large river catchments or entire river networks, the detection of groundwater inflow, even using natural tracers is problematic due to strong dilution, inhomogeneous mixing and resulting strong spatial variations and often also due to logistical problems (Dombrowsky, 2008; Neal et al., 2000; Rode and Suhr, 2007; Winter et al., 1998; Xie et al., 2016). Moreover, heterogeneity in tracer concentrations in the groundwater is also a major uncertainty at these scales because of changing landscape properties such as geology and sedimentology.

In 2018, Central Europe suffered from an extremely stable weather condition, resulting in the hottest summer season in eastern Germany since weather records began in 1881. The concurrent lack of precipitation, which was 28% below the long-term annual mean (DWD, 2019) resulted in extremely low flows in the Elbe River (minimum on 27. Aug. 2018: 136 m^3/s) at the Magdeburg gauge. As groundwater levels usually react to such short-term droughts with a delay, the situation was considered to be optimal for detecting groundwater inflows into the Elbe.

This study aims to localise and quantify groundwater discharge rates to a 1st order river system (Elbe River) by combining complementary approaches: i) by estimating hydraulic gradients between groundwater and river, divided by the distance ii) using mass balance and geochemical modelling of segments of the Elbe River and iii) highly spatially resolved 3 H measurements (~2 km) combined with a mass-balance model to provide the best possible and reliable quantification of groundwater inflow. The Elbe River (between the Czech-German border and Wittenberge, total length ~450 km) serves as a study area to apply the described multi-method approach, which is necessary to increase accuracy, validity and the understanding of complex flow systems (Bertrand et al., 2014). We are confident that the results will provide essential information for sustainable river management since the Elbe is a highly eutrophic river, which is a major cause of non-compliance with ecological quality standards under the European Water Framework Directive (WFD). The general approach may serve as a blueprint for other large river systems.

2. Study area

Our study area is a reach of the German Elbe River starting at the Czech-German border at Schmilka/Hřensko and ending 450 km downstream where the Havel joins the river at Wittenberge. From its source in the Giant Mountains (Czech Republic) to its mouth in the North Sea, the Elbe River drains an area of 150,000 km^2, making it one of the largest European rivers, passing through heterogeneous geological settings.

From Schmilka down to the City of Pirna, the river is deeply incised into the Cretaceous marl- and sandstones with several low conductivity aquifer stockworks (IKSE, 2005; Wilmsen and Niebuhr, 2014), which drain the Saxonian Sandstone Mountains predominantly through fault systems (Ad-Hoc-AG Hydrogeologie, 2016). Underlying aquifers are partly artesian and communicate with

the shallower ones. At Pirna, the landscape widens and is composed of low permeable Paleozoic metamorphic rocks before the river reaches downstream Dresden the Meißener Massif, consisting of low permeable magmatic rocks that drain Elbe-wards. Between Pirna and Riesa, up to 20 m thick Quaternary alluvial and glaciogenic/fluviatile deposits cover the Elbtal and host important porous aquifers. Wherever marly deposits cover the hard rock aquifers, the latter become locally confined. About 100 km away from the border, the river enters the North German Lowland, with its rather unconsolidated glacio-fluvial Quaternary sediments (Fig. 1) of which the uppermost two deposits of Saale and Weichsel Glacials are important aquifers (Eissmann, 2002). Here, the older Elster Glacial is of low permeability, but becomes an important sandy aquifer at Magdeburg, where shallow aquifers are often confined, even artesian, and also the deep groundwater drains towards the Elbe (Ad-Hoc-AG Hydrogeologie, 2016). Locally, groundwaters are saline due to ascending salt domes, penetrating the Tertiary Rupelton.

Hydrologically, the Elbe is a typical rain-snow type river. As a result of snowmelt in the late winter, the annual discharge maximum occurs in March and April, with an average of 850 m^3/s at the Magdeburg gauge (DGJ, 2014). Winter floods occur when intense and regional rainfall and snowmelt coincide, while summer floods are associated with specific weather situations (e.g. Vb-weather conditions), such as in August 2002 or in June 2013, when runoff at Magdeburg reached volumes of up to 5000 m^3/s (DGJ, 2014). However, regular summer discharge is less than 400 m^3/s at the same gauge (DGJ, 2014). Ecologically, the Elbe is a highly eutrophic river, with algal blooms occurring especially in the lowland parts and during droughts (Hardenbicker et al., 2016; Kamjunke et al., 2021).

3. Data and methods

In order to gain insight into both the location and quantification of groundwater discharge into the Elbe, a multi-method approach was applied. For the first, an analysis of hydraulic gradients was performed and for the second a differential flow gauging, an inverse geochemical modelling, a Darcy calculation and a numerical tritium mass balance model was used.

3.1. Water sampling

To identify the chemical and isotopic characteristics of the Elbe River and of the contributing end-members (rivers, groundwater and wastewater treatment plants) water samples were taken during several campaigns from (i) the Elbe River every 2 km, (ii) 14 of its major tributaries, (iii) the adjacent groundwater, and (iv) 11 major wastewater treatment plant effluents (WWTP). The sampling
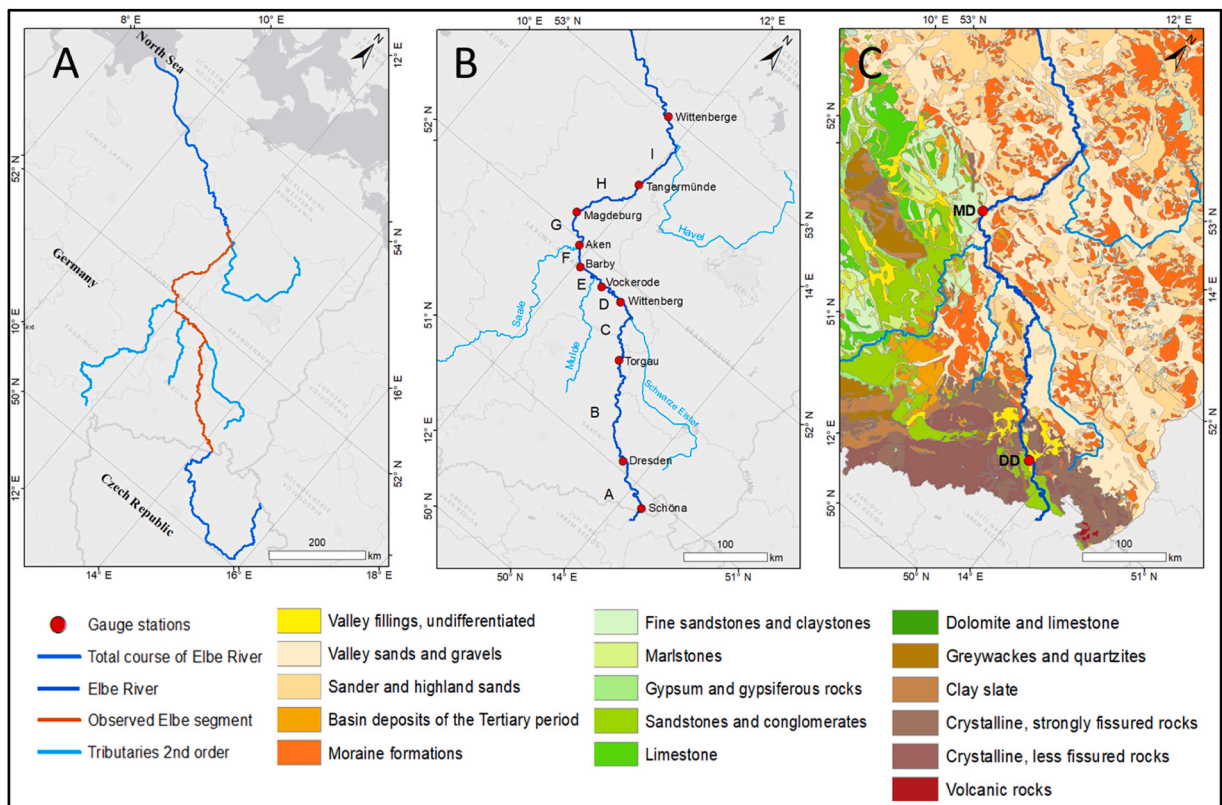
Fig. 1. Overview of the Elbe River study area. A) location within Europe B) study section showing the location of gauge stations and main tributaries in Germany and C) hydrogeological map along the studied Elbe part (ArcGIS, ESRI).

locations are listed in Table S2. To collect samples from the Elbe River, a Lagrangian sampling approach was employed by sampling from a boat that cruised faster than the river during daylight and stopped at night. Overall, we adhered to the travel time of the river for the observed stretch between Schöna to Havelberg, allowing to sample nearly the same water body downstream the river. Sampling was performed during Aug 13–21 2018 at extreme low flow conditions of 136 m³/s; this compares to a mean low summer discharge (MNQ) of 211 m³/s at Magdeburg gauge. Samples were taken close to the streambed every 2 km along the right-hand bank using a 5 L van Dorn sampler.

The major 14 tributaries were sampled at their inflow location. Groundwater samples from different aquifers were collected during the spring of 2020 from 29 wells along the right-hand bank of the Elbe River. Due to the lack of wells in the Saxonian Sandstone Mountains aquifer, samples were taken from 4 springs (locations are given in Table S2). Wells were pumped using a Grundfos MP1 submersible pump, and samples were taken after on-site parameters became constant and standing water has been exchanged 3 times. Effluents from the 11 largest WWTPs were sampled during autumn 2020 using a hand water sampler.

The on-site parameters (pH, T, EC, Eh) were determined for all samples with a WTW 350i instrument. Water samples for cations and anions were filtered (0.45 μm CA syringe filters) and separately filled into pre-cleaned HDPE containers. Cation samples were immediately acidified to pH less than 2 using concentrated HNO_3. Samples for tritium (^3H) were also collected into HDPE canisters. All samples were stored cool and dark before analyses in the laboratory.

Cations were analysed using ICP-OES (Optima 7300 DV, Perkin Elmer), while anions were determined using ion-chromatography (Dionex ICS-2000, Thermo Scientific). Bicarbonate was determined using gran-titration to an end pH of 4.3. ^3H samples were distilled and electrolytically enriched 12–15-fold in order to achieve ^3H accumulation. ^3H analyses were conducted by low background liquid scintillation counting (Hidex 300LS Hidex Oy, Finland, Tricarb 3180 PerkinElmer, USA) with a detection limit of about 0.08 Bq/l at the Federal Institute of Hydrology (BfG). All ^3H data are reported in Bq/l with a 2-sigma analytical uncertainty. All data are given in Tables S3 and S6.

3.2. Localisation of flux between groundwater and river

The hydraulic gradients were determined between wells and the Elbe River using the existing previously mentioned well network (all used wells are given in Table S1). To identify temporal changes in hydraulic gradients, the analyses were performed for the entire observed longitudinal profile of 450 stream km and a period of 9 years.

3.2.1. River stage

River stages [m.a.s.l.] were calculated every 500 m based on river stage time series [m above river bed] measured at 10 gauging stations (operated by Federal Waterways and Shipping Administration (WSV); Fig. 1B). These stations are ~1.2–44.7 km apart. The absolute river bed heights [m.a.s.l.] during the sampling campaign were determined every 500 m along the river from the Hydrax model (see sect. 3.3.4) (BfG, 2018). Water depth of the Elbe River at gauges is recorded on a daily basis. For the present study we use water depth data for each of the gauging stations from 01. Jan. 2010 – 31. Dec. 2018 (BfG, 2020).

Thereafter, resulting absolute river water levels for each time step were interpolated linearly between gauges to retrieve the required absolute river water level for each 0.5 river kilometre.

3.2.2. Groundwater level

Groundwater level data with variable sampling intervals were provided for the same period as river stage data (LfULG Saxony, 2020; LHW Saxony-Anhalt, 2020).

Data was collected from observation wells, located within 10 km from the Elbe River. There was no differentiation between wells penetrating deeper aquifers, which represent the regional flow field and wells drilled into the Quaternary aquifers, mainly showing local flow-fields.

Initially, each of the observation wells was assigned to the respective Elbe River kilometre using the Euclidean distance. Subsequently, out of these wells, only those wells were selected which have sub-monthly measurement intervals. The resulting list of wells is given in Table S1. To calculate hydraulic gradients on a daily basis, the groundwater level data have been downscaled to daily resolution linearly between the given time steps.

3.2.3. Derivation of hydraulic gradients between river and aquifer

To finally derive a hydraulic gradient I for each daily time step along the longitudinal profile of the Elbe River at 1 km resolution, we calculated the elevation differences between the Elbe River water level and the groundwater level for each time step and each well. Subsequently, and to obtain a comparable data basis among wells, results for each well were normalised given the flow length from the specific well to the Elbe River in the form:

$$I = \frac{h_{GW} - h_r}{L} \tag{1}$$

where I = hydraulic gradient, h_{GW} = groundwater level [m.a.s.l.], h_r = water level of Elbe River [m.a.s.l.], L = flow length as Euclidean distance of well to Elbe River [m].

3.2.4. Determining groundwater discharge locations from hydraulic gradients

Based on the hydraulic gradients, the obtained data sets consist of 173 hydraulic time series (Fig. 2). Each time series covers the time period of 2010–2018 with a daily resolution. With the intention to exclude any outlier due to short term effects (e.g. floods, heavy rainfall events, droughts), and measurements errors, we calculated the median of both, the entire time series and the campaign year 2018 for comparative reasons. Any resulting positive gradient represents a potential discharge of groundwater into the Elbe River. To emphasise the discharge likelihood we ranked the gradients along the entire longitudinal profile according to their frequency distribution in four classes: highly likely (>95th percentile), likely (≳95th - 75th percentile), probable (≳75th percentile but positive gradient), and unlikely (negative gradient).

Due to large depths to groundwater level in Saxonian Sandstone Mountains, the database is too poor along the first 30 km for a reliable analysis (Fig. 3).

## 3.3. Quantification of flux between groundwater and river

Effluent or influent conditions could be attributed to each river segment. While influent conditions were defined as a net loss of water from the river and quantified using differential gauging, groundwater discharge may result in a net gain of water. However, even segments with a negative balance may receive groundwater, while its amount does not compensate for loss but may change the resulting river water composition due to the delivered cocktail of dissolved components.

3.3.1. Flux balance (BAL)

Within our study area, the discharge of the Elbe River is regularly observed by the Federal Waterways and Shipping Administration (WSV) at 10 gauging stations (Fig. 2), subdividing the river into segments A to I (Table 1). For the period under study (Aug 13–21), gauging data from these stations have been averaged and applied to balance loss/gain of water within each segment. Along the
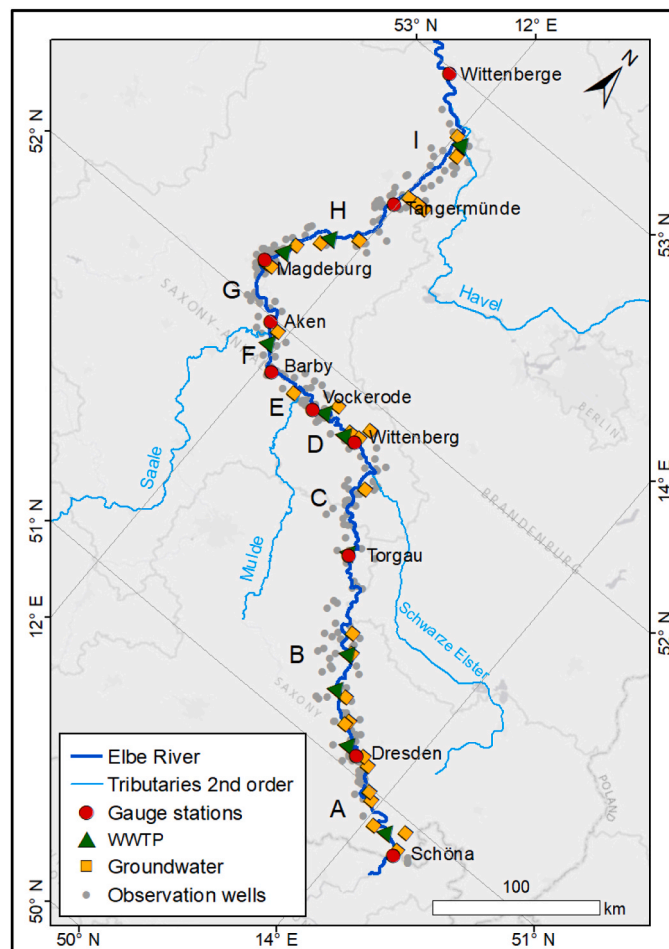
Fig. 2. Observation wells used for the analysis of hydraulic gradients and sampling locations for river-, ground-, tributary- and wastewater. Letters A-I indicate investigated river segments. (ArcGIS, ESRI).
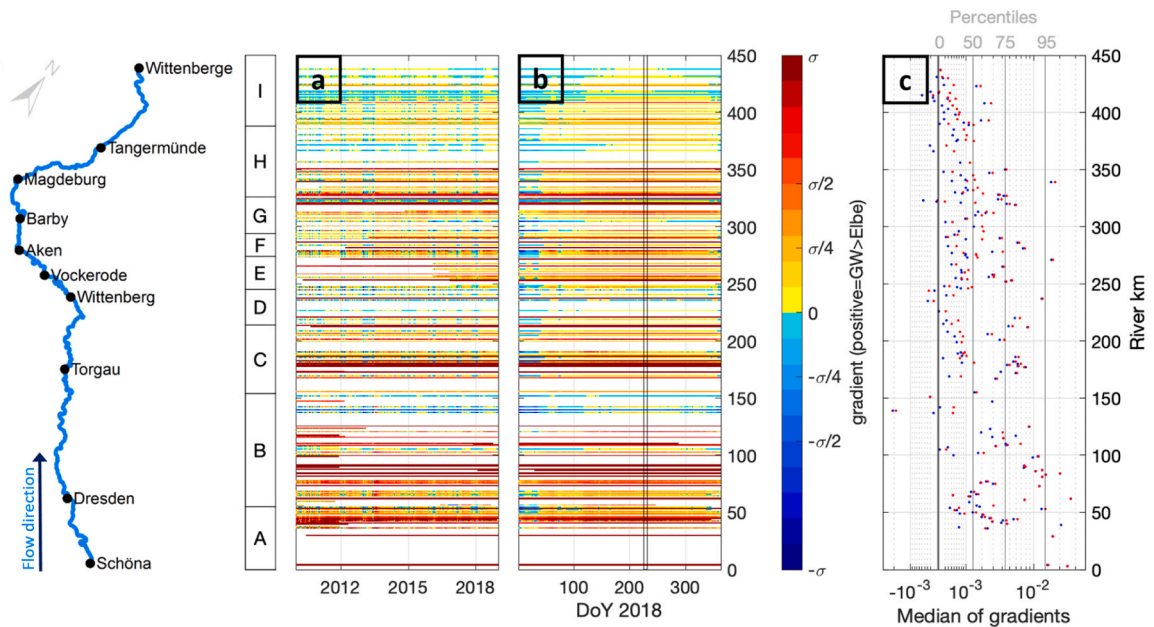
Fig. 3. Investigated reach of the Elbe River with gauging stations for illustration. The reach was divided into different segments A-I; a) normalised hydraulic gradients for a long-time period (01. Jan 2010–31. Dec 2018) and b) for the year 2018 (DoY=days of the year), including indication of field campaigns (two black vertical lines); c) Median of the hydraulic gradients for the long-term period 2010–2018 (blue dots) and for the reference period in 2018 (red dots) alongside the 50th, 75th and 95th percentiles for the median frequency distribution. High values indicate temporal stable hydraulic gradients.

segments, all inflows of rivers (Saale, Mulde, Schwarze Elster) and streams as well as of effluents from WWTPs have been considered (Tab. S4). The resulting volumetric difference either indicated net loss ($\Delta < 0$) or gain ($\Delta > 0$) of water, presumably groundwater.

To control the validity of the results, the chemical compositions of all (possibly contributing) sources i.e. (i) streams and rivers, (ii) WWTPs, (iii) groundwater wells along the river and (iv) the Elbe River at each gauging station were analysed. These data were taken to calculate molar ratios of Na/Cl and K/Br, assumed to behave inert with the water. The concept is as follows: if there is no contribution from any source, ratios must stay constant over the segment. In contrast, each discharge changes the chemical composition of the Elbe depending on the amount of water added. The chemistry of the known contributions from rivers, streams and WWTPs were included in the calculations. If an inflow of groundwater was accounted for, the corresponding molar ratios from the groundwater along the corresponding segment were used to calculate the hydrochemical composition of the Elbe at the end of the segment. If this agreed with an uncertainty of 10%, the balanced contribution from groundwater was assumed to be correct.

3.3.2. Geochemical modelling of water fluxes (GCM)

With this approach, the chemical composition of the Elbe River at the end of each segment A to I was considered to be the product of the Elbe water at the beginning of the segment and all known surface water and theoretically possible groundwater inflows along the respective segment. The latter were determined by applying the inverse modelling function of PhreeqC (Parkhurst and Appelo, 2013). Feeding the model with all observable chemical sources, it produces a set of possible mathematical solutions indicating the amounts and compositions of the missing water type, which is necessary to generate the chemical composition of the Elbe River at the segment's end. The subsequent selection process followed several principles: i) the simulated volumetric contribution of the Elbe River and of the contributing tributaries and WWTPs within the segment must resemble the real gauging data, ii) the sum of residuals should be minimised and iii) all phase mole transfers must be below 10^{-3}. If several model solutions fulfilled all aforementioned criteria, the model that exhibited the smallest sum of residuals and is closest to real measurements was finally chosen. The list of all river segments and the best three mathematical model solutions for each segment are given in Table S5.

3.3.3. Determination of flux from hydraulic gradients (DARCY)

The hydraulic gradients, which are calculated on a daily basis, and the location of the wells have been further used to estimate average groundwater flux to and from the river during the 9 days of sampling (Aug 13–21) according to the common Darcy approach:

$$Q = k_f \cdot A \cdot I \tag{2}$$

where k_f = hydraulic conductivity [m/s]; A = area, where the water must flow through to enter or leave the river [m^2], I = hydraulic gradient [-] taken from Eq. (1).

Hydraulic conductivity values (k_f) for the hydrogeological units, into which the boreholes were deepened, are taken from the

Table 1

List of Elbe segments, given by gauging stations along the river. Kilometration is given for the German river stretch, which starts briefly before Schöna at international Elbe km 370.7 at the Czech-German border. Given discharge is the average of daily measurements during our reference period (13–21 Aug 2018). Note that the ordering A to I is in the upstream direction for consistency with map representations. Fig. S7 shows a map of subcatchments for each segment.

Flow direction of Elbe River	Segment	Gauging stations	German river kilometration of gauging stations	Q [m³/s] at gauging stations	Segment length [km]	Segment Subcatchment [km²]
	I	Wittenberge	453.9	169	65.6	26.3
		Tangermünde	388.3	141		
	H	Tangermünde	388.3	141	61.6	4.03
		Magdeburg	326.7	142		
	G	Magdeburg	326.7	142	31.9	484
		Barby	294.8	141		
	F	Barby	294.8	141	20.1	24.7
		Aken	274.8	111		
	E	Aken	274.8	111	29.3	7.52
		Vockerode	245.5	95		
	D	Vockerode	245.5	95	31.4	692
		Wittenberg	214.1	94		
	C	Wittenberg	214.1	94	59.7	6.16
		Torgau	154.5	101		
	B	Torgau	154.5	101	98.9	2.12
		Dresden	55.6	87		
	A	Dresden	55.6	87	53.6	1.98
		Schöna	2.1	83		

hydrogeological map of Germany (BGR and SGD, 2016). To assign these values from the borehole to the interface section along the Elbe, where the water must flow through to enter or leave the river [m²], the midpoint of the way between the wells on each bank was determined. Then, the lengths of the two neighbouring bisectors of a well were summed up and multiplied with an average effective thickness of the interface. The effective thickness was taken from files of the WSV, made available via BfG and giving river depth at each 2nd river km.

3.3.4. Groundwater inflow estimated from tritium (^3H) mass balance modelling

High resolution ^3H sampling was used to quantify groundwater fluxes to the Elbe. The Elbe River contains highly elevated ^3H activities, which are derived from the Czech nuclear power plant (NPP) Temelín. The NPP is located at the banks of the Vltava River, ~225 km upstream of the confluence between the Vltava and Elbe Rivers. Dilution of riverine ^3H via groundwater discharge to the river was used to quantify the groundwater flux. The first sampling location (Schmilka) is about 350 river km downstream of the NPP, with NPP derived ^3H reaching the sampling location after ~3.3 days. Unfortunately, the fluxes and timing of ^3H releases from the NPP were not publicly available. During the five weeks prior to our sampling campaign, ^3H activities in the Elbe River at Schmilka varied between 6 and 8 Bq/l (recorded and provided by T. G. Masaryk, Water Research Institute).

Groundwater inflow rates can be estimated by inversely solving the river ^3H mass balance equation (Eq. 3). Eq. 3 was solved numerically by applying an implicit Petrov-Galerkin Finite Element scheme using a modified version of the software FINIFLUX, called TritiFLUX here (Frei and Gilfedder, 2015). TritiFLUX is a mass-balance model that was originally developed to quantify groundwater discharge to rivers and streams using radon (Cook et al., 2006; Frei et al., 2019; Frei and Gilfedder, 2015). The model is coupled to the optimization software BeoPEST (Doherty and Hunt, 2010) for the inverse estimation of groundwater inflow rates based on observed river ^3H activities. The reach specific groundwater discharge rates are systematically varied until the best fit is achieved between the simulated and measured ^3H activities. Optimization in BeoPEST was carried out using Tikhonov regularisation (Doherty and Hunt, 2010).

$$Q_s \quad \frac{dC}{dx} = I(C_{GW} - C) - dw\lambda C + \frac{Q_R}{R_L}(C_{trib} \quad - C) \tag{3}$$

Here, I [L^2/T] is the reach specific rate of groundwater inflow, Q_s [L^3/T] is the stream discharge, C [Bq/L^3] is the ^3H activity of the river, C_{GW} [Bq/L^3] is the ^3H groundwater end-member activity, d [L] is the mean river depth, w [L] is the width of river, $\lambda[1/T]$ the ^3H decay constant, Q_R [L^3/T] the inflow rate from tributaries, R_L [L] the tributary length at the confluence and C_{trib} [Bq/L^3] the ^3H activity of the tributary.

During the analysis, it was observed that there was only slow but progressive mixing between the Saale River, the largest tributary to the Elbe, and the Elbe River over ~50 km river length. This was due to the elevated salinity (density) in the Saale River, with an electrical conductivity (EC) of ~4.6 mS/cm at the confluence (see Fig. S10). In contrast, the Elbe River's EC was ~500 μS/cm. To account for this slow mixing of low ^3H Saale water into the main river, we used the EC in the Elbe River sample with the two end-member ECs to calculate the proportion of Saale water in the Elbe River sample. The dilution from the Saale water was then removed from the measured ^3H value so that we focus exclusively on dilution derived from groundwater. In addition, the Elbe River discharge was also corrected to only include the amount of Saale water contributing to ^3H transport, in a similar way to the ^3H value (c (^3H) Saale River = 0.62 ± 0.07 Bq/l).

The model input parameters further include the groundwater end-member (0.66 Bq/l), the length of each sub-reach (usually 2 km) and the mean width and mean depth of the reach. Morphological data such as river depth and width were provided by the WSV. River discharge was also measured by the WSV and was made available by the BfG. Discrete Q from the BfG for each 2 km reach was modelled with Hydrax (Oppermann et al., 2015). The depths and widths of the river were used to generate cross-sections by using elevation models.

Groundwater inflow rates for the Elbe River, based on the ^3H mass balance model, were determined according to the following assumptions:

(i) ^3H activities do not change in time (i.e. steady state).
(ii) There is no mechanism for ^3H activities to increase in the river, with changes only stemming from dilution. The model explicitly accounts for dilution by tributaries based on linear-mixing between tributary and river end-members and river flow.
(iii) The groundwater end-member (C_{GW}) was defined as the mean ^3H activities of 27 groundwater samples collected from shallow aquifer sections close to the river. Based on these data C_{GW} was set uniformly to 0.66 Bq/l for the entire Elbe River. This groundwater end-member was used for all model calculations.
(iv) The activities at each sampling point (see S6) are representative for the whole sub-reach at the sampling location.
(v) As no precipitation fell during and before the sampling campaign, rain was not considered influential in this study.

4. Results

4.1. Localising of flux between groundwater and river

As described above, the lack of groundwater level information in the Sandstone Mountains prevents a sound interpretation of hydrological gradients in the first 30 km of the investigated section of the Elbe River (Fig. 3). However, the locations and altitudes of springs along this stretch of the river indicate steep gradients towards the Elbe. Analyses of hydraulic gradients along the studied reaches of the Elbe indicate that some reaches were influent (Elbe water discharges into the adjacent aquifer) and others are predominantly effluent (groundwater discharges into the Elbe). Although natural heterogeneity of the aquifer hydraulic properties (kf) and the cross-sectional area control the flow, the discharge either into or from the river increases with the gradients.

Fig. 3a shows the calculated hydraulic gradients for almost a decade (2010–2018) and an additional plot for the year 2018 in Fig. 3b. The y-axis indicates the different stream segments (A-I) for which hydraulic gradients have been estimated. The colour of the bands indicates either effluent (reddish) or influent (blueish) conditions, with sigma representing the variance of all gradients. Almost everywhere along the river, hydraulic gradients vary considerably and the direction of exchange is even reversed seasonally for many segments. While effluent conditions dominate between early summer and autumn, the typical high-flow regime in winter and spring leads to the reversal of the gradients and influent conditions during these months. However, a significant number of locations along the river are characterised by constant positive gradient (continuous red lines in Fig. 3a, b coincide with values above the 75th percentile in Fig. 3c), indicating permanent groundwater discharge conditions. Permanent groundwater discharge occurs predominantly for the upstream segments A and B and decreases further downstream. This can be explained by the flattening of the landscape topography.

The drought year 2018 started with an exceptionally wet January (Fig. S8), resulting in predominantly influent conditions during the first 30 days (indicated by the bluish colours during the first 30 days of the year in Fig. 3b). After this initial period, exchange rapidly changed into effluent conditions (yellow to red colours), which persisted for the remainder of the year.

For segments with large gradients (>75th percentile Fig. 3c), the temporal variability is less pronounced as the differences tend to be stable over time. While the gradient alone is an indicator of likely groundwater discharge and temporal hydraulic stability, the gradient remains qualitative and does not provide any quantitative data on groundwater discharge volumes.

4.2. Quantification of flux between groundwater and river

4.2.1. Estimation of potential Darcy-flux (DARCY)

The result of the Darcy calculation was a total groundwater discharge of 13.1 m^3/s over the 450 river km. Though hydraulic gradients from groundwater to the river are large (Fig. 3), the low hydraulic conductivities of rocks in the Saxonian Sandstone Mountains results in a calculated inflow in segment A of 0.5 m^3/s only, while the effluent flow increases in the following reaches B and C, to 4.4 and 4.7 m^3/s, respectively. With the downstream flattening of the landscape, hydraulic gradients decrease more and more, resulting in low groundwater inflow of 0.2–0.7 m^3/s in the subsequent segments D-I, with the exception of segment G, where 1.4 m^3/s of groundwater enters the river.

4.2.2. Flux balance (BAL)

Groundwater inflow rates calculated using the differential gauging method are shown for each segment in Fig. 4. The largest groundwater contributions occur in segments A, B, E and I, while other segments show low inflow rates (D and G) or no total contribution (C, F, H). The total groundwater volume that entered the Elbe along the 450 km reach studied here was 34.2 m^3/s, which represents 28.7% of the total Elbe River discharge at the Wittenberge gauge and 41.8% of all inflow components. In addition to the groundwater contribution, Fig. 4 also illustrates the occurrence and magnitude of surface inflow contributions from WWTPs (B, E, H), and tributaries (A, B, C, E, F, H, I). While the majority of the segments show a positive water balance (effluent reaches), three segments (C, F, H) show partially net influent conditions with a net negative water balance.

The absolute errors in Fig. 4 are based on an estimated relative error of 5% for each discharge value from the gauging stations (IKSE, 2005). In view of the large errors resulting from this approach, we further consolidate the mass balance indications with the inverse geochemical modelling for aqueous systems.

4.2.3. Inverse geochemical modelling (GCM)

The results of the chemical mass-balances conducted in PHREEQC are shown in Fig. 5. The fluxes shown are normalised to the river discharge at the end of the respective segment. While the river discharge is shown in blue, the contributing components (surface and groundwater inflow) are shown in green colours. The relative groundwater contributions vary greatly over the 450 km reach of the Elbe River. The simulated relative groundwater contributions were highest for the segments A and I (≳10% of river flow), moderate for the segments B, C and E (3.0–3.1%), and lowest for segment G (0.7%). Along the segments D, F and H, groundwater inflows are either absent or too low to influence the chemical composition of the river.

In addition, three segments (B, C, H) show significant contributions from WWTPs (%), and segments C, E, G and I receive large inflows from tributaries (%). As a result of the inverse modelling, a total groundwater contribution of 37.4 m^3/s (31.1% of the total
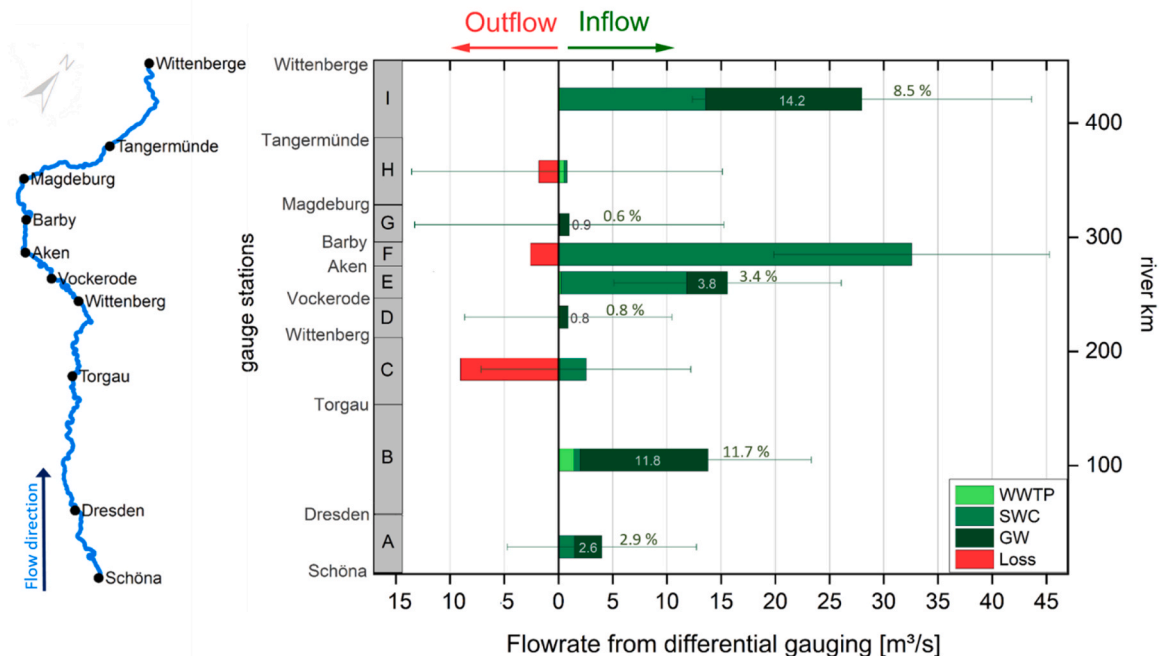

Fig. 4. Results for flux balance of inflow (red) and outflow (greenish) components to Elbe River during the reference period (Aug 2018) when the river stage was lowest (WWTP = wastewater treatment plant, SWC = surface water contribution, GW = groundwater). Fluxes below 0.2 m^3/s are not shown in the figure. Absolute errors are given in green bars. Elbe River is given for illustration.
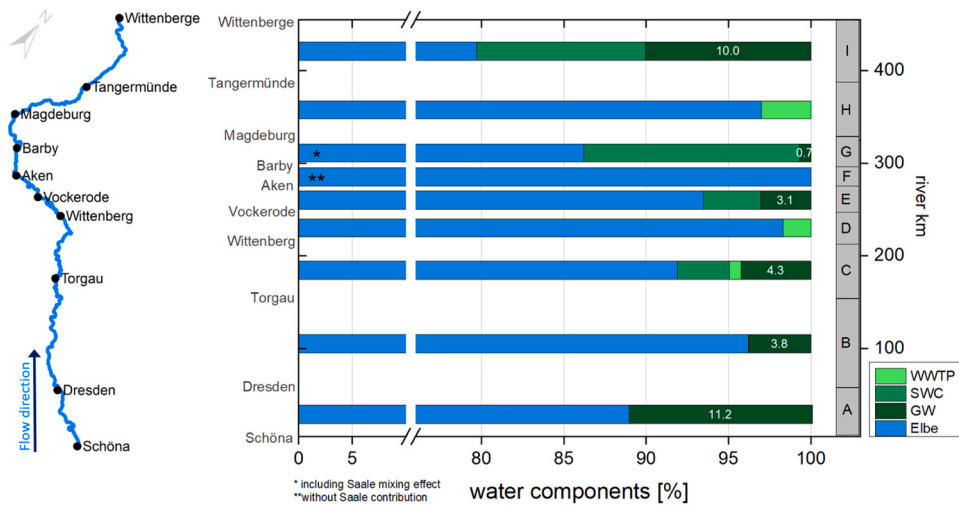
Fig. 5. Results of the inverse geochemical modelling of the Elbe River during the reference period (Aug 2018) (WWTP = wastewater treatment plant, SWC = surface water contribution, GW = groundwater); Note: (1) line break on x-axis for better presentation of inflow components; (2) River Saale as major contributor enters the Elbe in segment F approximately before the end of the segment at Barby gauging station and on the left bank, while samples were consequently taken at the right bank in the Elbe River (ca. 180 m wide at Barby). Hence, the impact of Saale water was chemically noticeable in the G-segment only. Elbe River is given for illustration.
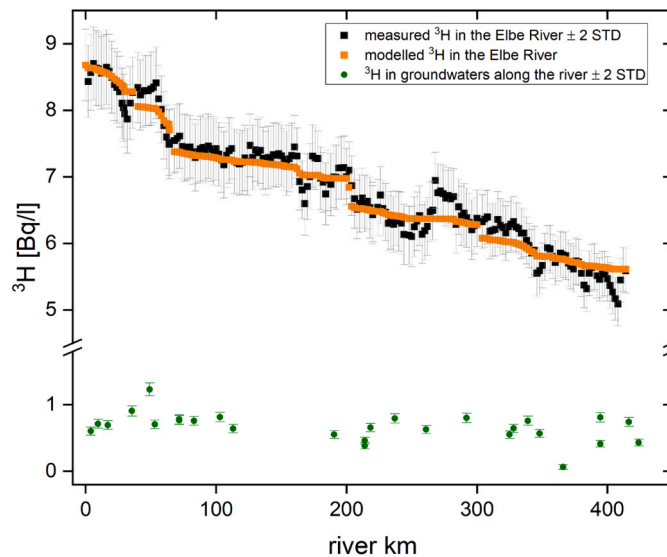
Fig. 6. Determined measured (black) and modelled (orange) ^{3}H activities in river water and in groundwater (green) along the Elbe River. Note: line break on y-axis.

discharge at the Wittenberge gauge) was estimated along the study reach of the Elbe River.

4.2.4. Tritium dilution modelling (^{3}H)

Dilution of anthropogenic ^{3}H in the Elbe River (originating from the Temelín NPP) by surface- and low-tritium groundwater inflows was used to quantify the sub-reach specific groundwater inflow rates. This concept is based on (i) the assumption of a constant ^{3}H input value at the upstream end of the investigated Elbe River section (approx. 8.0 Bq/l, table S6) and (ii) the Lagrangian sampling approach used here (see sect. 3.1). As there are no ^{3}H sources other than the NPP, the model is unable to simulate an increase in ^{3}H activities downstream of the source. However, as illustrated in Fig. 6, increasing ^{3}H activities were measured for some sub-reaches. It can also be seen that such increases are generally followed by a rapid decrease in the ^{3}H activity. This pattern of increasing and decreasing ^{3}H activities can be explained by incomplete mixing of water in the river channel and where samples were taken at different locations across the channel. Hence, the increases which are followed by decreases in the ^{3}H activities reflect the recovery of the ^{3}H activity in the sampled river water after completely mixing a few sampling stations downstream.
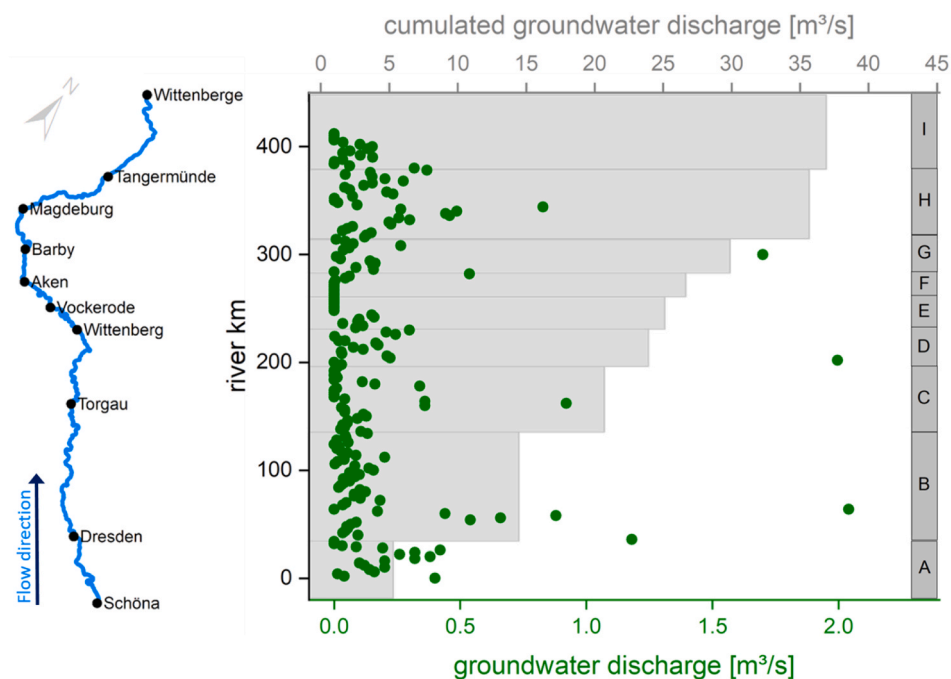
Fig. 7. [3]H mass balance modelled groundwater inflow into the Elbe River. Note that the lower green x-axis refers to all green points (discrete groundwater discharge) while the upper grey x-axis refers to the grey bars (cumulative groundwater discharge) in the figure. Segments A-I on the right y-axis are given for illustration.

At the upstream end of the study reach, which was the start of our campaign, ^{3}H activity in the Elbe River were 8 Bq/l, which was significantly higher than both the ^{3}H activities in groundwater (0.4–1.2 Bq/l (Table S6)) and the natural background in precipitation in the Elbe catchment (0.5–1.1 Bq/l for the time period 2015–2022 at GNIP stations Berlin, Germany and Uhrliska, Czech Republic (Schmidt et al., 2020)). Hence, the dilution of the ^{3}H activities along the river could be quantitatively associated with groundwater and surface water inflow into the river. Generally, ^{3}H activities gradually decreased along the entire 450 river km from 8.4 ± 0.57 Bq/l to 5.5 ± 0.33 Bq/l (Fig. 6). The simulated ^{3}H values (based on the ^{3}H mass balance model) generally followed the dynamics of the measured ^{3}H activity in the river (Fig. 6). For the entire reach, the simulated values approximated the measured ^{3}H values very well (R^2 = 0.913, $p < 0.001$). Fig. 7 illustrates the modelled groundwater inflow into the Elbe River based on the ^{3}H mass balance model. Total accumulated groundwater inflow for the investigated Elbe River reach was calculated to be ~37.7 m^3/s, representing 38.2% of the total river discharge at the downstream end of the investigated river reach (Havel River confluence). Along 60% of the entire reach (in total 122 sub-reaches of each 2 km), simulated groundwater inflow rates were below 0.10 m^3/s. Groundwater inflow rates exceeded 0.5 m^3/s at 10 sub-reaches (representing only 4.9% of all 206 modelled sub-reaches). The highest groundwater inflow rates were simulated at km 36, 64, 202, and 300 with inflow rates of 1.18, 2.04, 1.99 and 1.70 m^3/s, respectively (Fig. 7).

5. Discussion

Our results indicate that groundwater discharge occurs along the entire 450 km reach of the Elbe River, while there is a significant zonation with certain regions having a higher probability of groundwater discharge compared to others (Fig. 8 and S9).

For the first 210 river km (segments A-C), the results of the applied methods are consistent, and indicate a total groundwater discharge of 9.6–22.9 m^3/s. Along this reach, the hydraulic gradients in almost 40% of the wells (i.e. 13 from a total of 33 wells) are oriented towards the Elbe and highly effluent (>75th percentile), indicating a persistent groundwater discharge. Floods as short-term events may reduce the magnitude of groundwater discharge, but not reverse the direction of flow in these regions for a long period or over a large area (Fig. 3). There are no groundwater wells in the Saxonian Sandstone Mountains over the 30 km study reach. However, perennial springs a few tens of metres above the Elbe River indicate large and similarly stable hydraulic gradients towards the river. Groundwater flow in this aquifer occurs predominantly along faults and fractures, which may support the assumption that groundwater inflow to the Elbe is localised, while low transmissivities prevent significant diffuse inputs by matrix flow (Ad-Hoc-AG Hydrogeologie, 2016; Brodie, 2007; Hassan et al., 2014).

In segment B, all methods indicate a similar quantity of groundwater discharge as in the first segment. In contrast, the results for the ~60 km long segment C vary considerably depending on the method used. While inverse geochemical (GCM), ^{3}H modelling as well as the Darcy approach result in inflow rates of 2.8, 7.1 and 4.7 m^3/s, respectively, the differential gauging results in a net water loss of about − 9.0 m^3/s. This river section is unique in that in the last 10 km of segment B (km 145) and especially in the first 25 km of segment C, the Torgau waterworks carry out intensive bank filtration, artificially creating negative hydraulic gradients and thus the
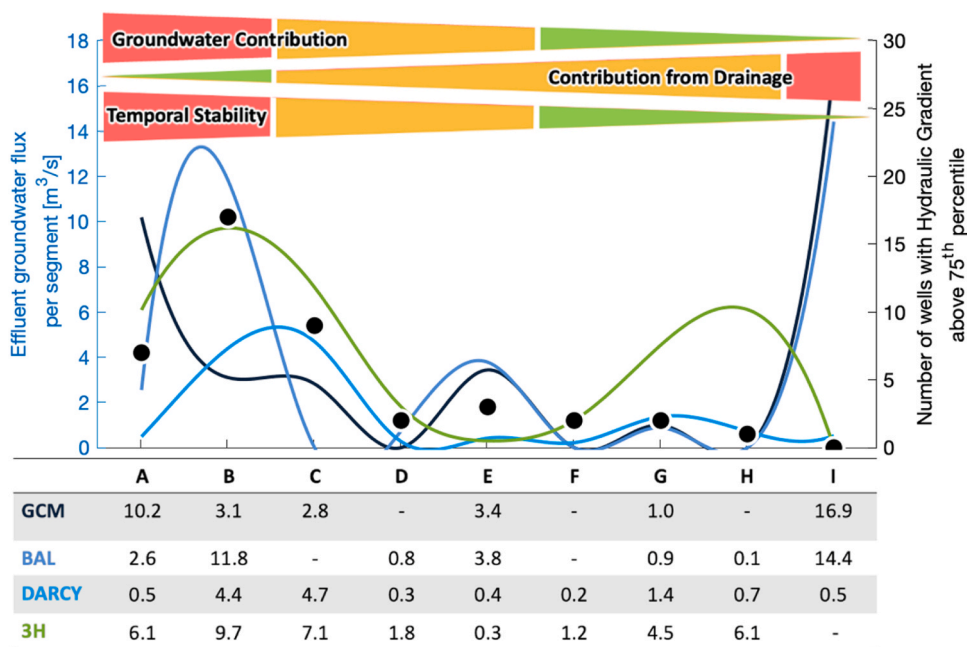
Fig. 8. Combined interpretation of qualitative and quantitative approaches for all investigated Elbe segments. Besides its interpretation regarding groundwater contributions, temporal stability and the deduced contribution from field drainages as an outcome of the diverging results of a) BAL/ GCM/3 H (all three based on geochemistry and measured water volumes) and b) DARCY/the number of wells with hydraulic gradients above the 75th percentile (both based on water level data). Note that the left blue ordinate axis refers to all line elements while the right black ordinate axis refers to point elements in the figure.

Elbe to loses water to the aquifer. Further downstream but still within the same segment (last 35 km), conditions revert to those of a gaining river, with sufficient groundwater flowing into the Elbe to modify the river chemistry. It was not sufficient, however, to compensate for the amount of water abstracted by the water works, resulting in a net losing reach.

In the region of Lutherstadt Wittenberg, the Elbe enters the North German Lowland with its flat topography. From this point the hydraulic gradients were small (only 3 wells show gradients >75th percentile) and the groundwater discharge in segments D and E is correspondingly low (approx. 0.3–0.4 m^3/s according to the Darcy calculations) (Figs. 3, 8). However, volumetric balancing (BAL), inverse modelling (GCM) and ^{3}H dilution modelling (^{3}H) indicate a groundwater discharge of 0.8–3.8, 0–3.4 and 0.3–1.8 m^3 /s, respectively (Figs. 4, 5 and 7). At the transition from D to E, the hydraulic gradients oscillate around zero (Fig. 3), indicating flow directions between the aquifer and the river that have a low temporal constancy and are highly sensitive to droughts and floods with rapidly changing river stages. During our observations, groundwater level had not yet responded to the prevailing drought conditions, resulting in groundwater discharge that could be much lower or even influent under regular conditions.

At the same time, the frequent changes of in- and effluent conditions also mean that the river banks are either drying or rewetting, creating a bank storage situation alongside the land-water interface (McCallum et al., 2010). In areas of bank storage, reactive solutes from groundwater and river water (including nutrients and dissolved organic carbon) can undergo biogeochemical transformations mediated by microbial activity (Gu et al., 2012). Such responsive areas can determine the final fluid composition of the water discharged into the Elbe during dry periods and may be important hotspots for transformation processes in the river. In addition, Elbe sediments are constantly being desiccated and rewetted by oscillations in the river level, which can lead to a burst of decomposition and mineralisation including the release of bioavailable P (Kerr et al., 2010), inorganic nitrogen and CO_2 (Jarvis et al., 2007; Mallast et al., 2020). Such processes are likely to affect water quality in the Elbe.

These transformation effects may increase downstream in segments F-H, where hydraulic gradients decrease further and the contribution of groundwater decreases to 0–6.1 m^2/s (Figs. 3, 8). In the area from river km 320–330, the hydraulic gradients are exceptionally high (between the 50th and 75th percentiles and even higher (Fig. 3c)), indicating the area with the highest discharge rates. ^{3}H modelling also identifies high groundwater contributions at river km 328–344 (Fig. 7). However, cumulative errors in the volumetric balance (Fig. 4) introduce uncertainties into groundwater input rates in this area. All four approaches show comparatively low groundwater inputs along segments F to H of the Elbe River (Fig. 8). Instead, WWTPs and surface runoff contribute 1% and 13% (GCM in Fig. 5) or 0.4% and 23% (BAL in Fig. 4) of the total river discharge, respectively, and dominate the water input to the Elbe.

The final segment of the Elbe River shows unexpected results. Although kf-values are high (10^{-3} - 10^{-2} m/s), the negligible hydraulic gradients result in minimal Darcy flow of groundwater (0.5 m^3/s) into the Elbe (Fig. 8). In contrast, the BAL and GCM methods (Fig. 8) indicate much higher groundwater contributions of 14.4 and 16.9 m^3 /s, respectively. These figures represent 8.5% and 10% of the total flow in the final segment, and are similar high to those in the upstream segments A and B and are much too high given the low hydraulic gradients. The ^{3}H approach can not be used purposefully here, since only the first 35% of the whole segment I was sampled.

The large discharge of water entering the Elbe may be due to the extremely dense and extensive network of drainage ditches surrounding the Elbe in this part of the catchment (LfULG Saxony, 2013; LLG Saxony-Anhalt, 2021). Given the exceptionally low water level of the Elbe at the time of sampling, the drainage ditches may drain the surrounding landscape much more efficiently than under normal conditions. As with groundwater, these ditches transport dissolved solids, nutrients (P, N, C) and pesticides from agricultural areas into the river (Blann et al., 2009). Consequently, the apparently large volume of drainage water leads to significant changes in river hydrochemistry (GCM) and increased discharge rates (BAL) at the end of segment I. As the drainage systems are piped, DARCY, on the other hand, could not account for this leading to the low Darcy-based discharge estimates. Nevertheless, this part of the Elbe may be particularly important for the water quality. While the direct contributions of groundwater is rather negligible or even absent during wetter periods, the contribution of agricultural drainage increases and directly links agricultural land use to the water quality of the Elbe. This is not unique to the present study area (King et al., 2014; Pavelis et al., 1987). Although another link between the two is groundwater, field drainage is similar to a rapid and unfiltered pathway (Smith et al., 2015) which may have a greater impact on Elbe water quality in this area than groundwater (Gilliam et al., 1999; Skaggs et al., 1994). With an increasing number of hydrological droughts in the future, this input in particular will recur at regular but increasing intervals (Prudhomme et al., 2013).

6. Conclusion

This study contributes to the identification and quantification of diffuse groundwater discharge and thus to the currently poorly delineated sources of nutrients (N, P) and other solutes in the Elbe River (Donohue et al., 2005; Sharpley et al., 1994; UBA, 2020). The use of several independent methods to determine groundwater discharge volumes and composition has proved reasonable. No single method has been able to provide conclusive results, but together they provide an estimate and quantifiable uncertainty of the groundwater flux. Pure balancing is unable to distinguish groundwater discharge in segments with a negative total water balance. These can only be detected using chemical or isotopic tracers. At the same time, smaller amounts of groundwater in a system like the Elbe River do not necessarily lead to significant changes in the major element composition of the river. The activity of ^{3}H, on the other hand, provides a sensitive hydrological tracer that shows a significant decrease due to the dilution effect of groundwater. Moreover, ^{3}H is conservative and part of the water molecule, making its interpretation simpler than other reactive chemical species. The evaluation of the hydraulic gradients and the spatial occurrence of the discharge conditions is sensitive to a series of effects. The natural heterogeneity in the hydraulic conductivity of the adjoining aquifer can vary by orders of magnitude over short distances, which is not resolved in any dataset, particularly not those on a national scale. In the downstream lowland reaches of the Elbe River, flat or even horizontal hydraulic gradients quickly react to precipitation events, local and remote ones, in headwater catchments. They change gradients between the Elbe and the groundwater as short to mid-term responses. And last but not least, both approaches are inapplicable to verify the contribution of artificial drainage networks.

It can be concluded, to determine groundwater inflow along a large, first order river system, which flows through an intensely manufactured cultural landscape, a single method may fail, while a combination of independent and complementary methods might be appropriate. As a result, we were able to estimate groundwater discharge rates that can be used to quantify matter inputs. In addition, our multi-method approach provides, for the first time, a way to detect and assess the impact of drainage channels in a large river system such as the Elbe. Although their existence is generally known, documents on the form and extent of the drainage network were lost during the political upheavals in the former East Germany in the early 1990 s. However, it is important to identify field drains and their impact on water quantity as it may be another significant source of chemical inputs. As they transfer agrochemicals to surface water bodies without any retention (e.g. as may occur in the aquifer), field drains are likely to have a much greater impact on the ecological status of the Elbe River than other sources, especially during low-flow conditions, which may become more frequent in future summer seasons (IPCC, 2018). According to international conventions, the resulting nutrient loads in waterways must be halved by 2030 at the latest compared to 1985 concentrations (HELCOM, 2021; OSPAR, 2021). The quantitative information provided here, as well as information on sources and associated pathways, is therefore essential and can contribute to sustainable river basin management.

In particular, the identification of the drainage contribution highlights the importance of using a multi-method approach. While the long-term, high-resolution analysis of hydraulic gradients along the river allows one to pinpoint groundwater discharge locations and their temporal constancy, all four quantitative approaches (inverse geochemical and ^{3}H modelling, flux balances and Darcy) provide integral information about the flow rates of discharging groundwater in an observed segment. More importantly, the examination of different modelling trends over the longitudinal profile of the river reveals different sources of fluxes (groundwater vs. drainage) that would not have been identified using only one approach. In other words, the combination of models is the key to understanding large-scale systems with a huge number of potential and interacting processes and contributors, which are usually masked by high dilution.

The two complementary results, localisation and quantification, provide essential information for sustainable river management as required by the European Water Framework Directive (WFD). Eutrophication is now a major cause of non-compliance with ecological quality standards under the WFD and other international river basin management directives. The Elbe is a model river in which limiting nutrients can be completely converted into algal biomass during peak events (Kamjunke et al., 2021). It is therefore crucial for managers to properly identify nutrient sources, and groundwater inputs often remain a 'black box'. Our combined approach fills this gap and may serve as a blueprint for other large river systems.

CRediT authorship contribution statement

Schmidt Axel: Formal analysis. **Gilfedder Benjamin S.:** Formal analysis, Validation, Writing – original draft, Writing – review &

editing. **Rödiger Tino:** Conceptualization, Writing – original draft. **Zill Julia:** Data curation, Formal analysis, Funding acquisition, Project administration, Software, Validation, Visualization, Writing – original draft, Writing – review & editing. **Siebert Christian:** Conceptualization, Methodology, Supervision, Writing – original draft, Writing – review & editing. **Frei Sven:** Formal analysis, Software. **Schubert Michael:** Formal analysis. **Weitere Markus:** Conceptualization, Writing – original draft. **Mallast Ulf:** Data curation, Formal analysis, Software, Supervision, Visualization, Writing – original draft, Writing – review & editing.

Declaration of Competing Interest

Data availability

All data are given in the Supplementary index.

Acknowledgements

Financial support

Appendix A. Supporting information

Supplementary data associated with this article can be found in the online version at doi:10.1016/j.ejrh.2023.101595.

References

Ad-Hoc-AG Hydrogeologie: Regional Hydrogeology of Germany: Aquifers in Germany, their distribution and properties, Geol. Jb., A 163: 456, Hannover, 2016.

Bachmann, R., 1980. The role of agricultural sediments and chemicals in eutrophication. J. Water Pollut. Con F. 52, 2425–2600.

Bertrand, G., Siergieiev, D., Ala-Aho, P., Rossi, P.M., 2014. Environmental tracers and indicators bringing together groundwater, surface water and groundwater-dependent ecosystems: importance of scale in choosing relevant tools. Environ. Earth Sci. 72, 813–827. https://doi.org/10.1007/s12665-013-3005-8.

BfG: Sole highs and river width data in an equidistance of 0.5 km during August 2018, Federal Institute of Hydrology (BfG) division G4 "Radiology and Water Monitoring", 2018.

BfG: Runoff and water level data of the Federal Waterways and Shipping Administration (WSV), provided by the Federal Institute of Hydrology (BfG) division M1 "Hydrometry and Hydrological assessment", 2020.

BGR and SGD: Federal Institute for Geosciences and Natural Resources (BGR) and State Geological Services (SGD), Hydrogeological Overview Map of Germany 1: 200,000, Upper Aquifer (HÜK200 OGWL), digital dataset, version 3.0. - Hannover, 2016.

Blann, K.L., Anderson, J.L., Sands, G.R., Vondracek, B., 2009. Effects of agricultural drainage on aquatic ecosystems: a review. Crit. Rev. Env Sci. Tec. 39, 909–1001. https://doi.org/10.1080/10643380801977966.

Botting, J., 2010. Groundwater flow patterns and origin on the North Bank of the Wairau River, Marlborough, New Zealand, M.Sc. in. Engineering Geology. University of Canterbury,, Christchurch, New Zealand.

Bouza-Deaño, R., Ternero-Rodríguez, M., Fernández-Espinosa, A.J., 2008. Trend study and assessment of surface water quality in the Ebro River (Spain). J. Hydrol. 361, 227–239. https://doi.org/10.1016/j.jhydrol.2008.07.048.

Bowes, M.J., Armstrong, L.K., Harman, S.A., Wickham, H.D., Nicholls, D.J.E., Scarlett, P.M., Roberts, C., Jarvie, H.P., Old, G.H., Gozzard, E., Bachiller-Jareno, N., Read, D.S., 2018. Weekly water quality monitoring data for the River Thames (UK) and its major tributaries (2009–2013): the Thames Initiative research platform, Earth Syst. Sci. Data 10, 1637–1653. https://doi.org/10.5194/essd-10-1637-2018.

Brodie, R., Sundaram, B., Tottenham, R., Hostetler, S., Ransley, T., 2007. An Overview of Tools for Assessing Groundwater-Surface Water Connectivity. Australian Government, Bureau of Rural Sciences, Canberra, Australia.

Brookfield, A.E., Hansen, A.T., Sullivan, P.L., Czuba, J.A., Kirk, M.F., Li, L., Newcomer, M.E., Wilkinson, G., 2021. Predicting algal blooms: are we overlooking groundwater? Sci. Total Environ. 769, 144442 https://doi.org/10.1016/j.scitotenv.2020.144442.

Brunke, M., Gonser, T., 1997. The ecological significance of exchange processes between rivers and groundwater. Freshw. Biol. 37, 1–33. https://doi.org/10.1046/j.1365-2427.1997.00143.x.

Burbery, L., Ritson, J., 2010. Integrated study of surface water and shallow groundwater resources of the Orari catchment, RNo10/36. Environment Canterbury Regional Council, Christchurch, New Zealand.

Cantafio, L.J., Ryan, M.C., 2014. Quantifying baseflow and water quality impacts from a gravel-dominated alluvial aquifer in an urban reach of a large Canadian river. Hydrogeol. J. 22, 957–970. https://doi.org/10.1007/s10040-013-1088-7.

Chapman, D.V., Bradley, C., Gettel, G.M., Hatvani, I.G., Hein, T., Kovács, J., Liska, I., Oliver, D.M., Tanos, P., Trásy, B., Várbíró, G., 2016. Developments in water quality monitoring and management in large river catchments using the Danube River as an example. Environ. Sci. Policy 64, 141–154. https://doi.org/10.1016/j.envsci.2016.06.015.

Cheng, C., Song, J., Chen, X., Wang, D., 2010. Statistical distribution of streambed vertical hydraulic conductivity along the Platte River, Nebraska. Water Resour. Manag. 25, 265–285. https://doi.org/10.1007/s11269-010-9698-5.

Close, M., Knowling, M., Moore, C., 2016. Modelling of Temperature in Wairau Aquifer. Institute of Environmental Science and Research Limited (ESR), CSC 16007. Marlborough District Council,, New Zealand.

Coluccio, K., Morgan, L.K., 2019. A review of methods for measuring groundwater–surface water exchange in braided rivers. Hydrol. Earth Syst. Sci. 23, 4397–4417. https://doi.org/10.5194/hess-23-4397-2019.

Cook, P.G., 2013. Estimating groundwater discharge to rivers from river chemistry surveys. Hydrol. Process. 27, 3694–3707. https://doi.org/10.1002/hyp.9493.

Cook, P.G., Favreau, G., Dighton, J.C., Tickell, S., 2003. Determining natural groundwater influx to a tropical river using radon, chlorofluorocarbons and ionic environmental tracers. J. Hydrol. 277, 74–88. https://doi.org/10.1016/S0022-1694(03)00087-8.

Cook, P.G., Lamontagne, S., Berhane, D., Clark, J.F., 2006. Quantifying groundwater discharge to Cockburn River, southeastern Australia, using dissolved gas tracers ^{222}Rn and SF$_6$. Water Resour. Res.. 42, W10411. https://doi.org/10.1029/2006WR004921.

Dodds, W.K., 2006. Eutrophication and trophic state in rivers and streams. Limnol. Oceano 51, 671–680. https://doi.org/10.4319/lo.2006.51.1_part_2.0671.

Dodds, W.K., Bouska, W.W., Eitzmann, J.L., Pilger, T.J., Pitts, K.L., Riley, A.J., Schloesser, J.T., Thornbrugh, D.J., 2009. Eutrophication of U.S. Freshwaters: analysis of Potential Economic Damages, Kansas State University, Manhattan, Kansas. Environ. Sci. Technol. 43, 12–19. https://doi.org/10.1021/es801217q.

Doherty, J.E., Hunt, R.J., 2010. Approaches to highly parameterized inversion—A guide to using PEST for groundwater-model calibration. U. S. Geol. Surv. Sci. Investig. Rep. 59, 2010–5169. ⟨https://pubs.usgs.gov/sir/2010/5169/⟩.

Dombrowsky, I., 2008. Institutional design and regime effectiveness in transboundary river management – the Elbe water quality regime. Hydrol. Earth Syst. Sci. 12, 223–238. https://doi.org/10.5194/hess-12-223-2008.

Donald, D.B., Bogard, M.J., Finlay, K., Bunting, L., Leavitt, P.R., 2013. Phytoplankton- specific response to enrichment of phosphorus-rich surface waters with ammonium, nitrate, and urea. PLOS ONE 81, e53277. https://doi.org/10.1371/journal.pone.0053277.

Donohue, I., Styles, D., Coxon, C., Irvine, K., 2005. Importance of spatial and temporal patterns for assessment of risk of diffuse nutrient emissions to surface waters. J. Hydrol. 304, 183–192. https://doi.org/10.1016/j.jhydrol.2004.10.003.

DWD: German weather service, monthly weather description of the year 2018: https://www.dwd.de/DE/leistungen/pbfb_verlag_monat_klimastatus/monat_klimastatus.html, last access: 20. September 2019.

Eissmann, L., 2002. Quaternary geology of eastern Germany (Saxony, Saxony–Anhalt, South Brandenburg, Thüringia), type area of the Elsterian and Saalian Stages in Europe. Quat. Sci. Rev. 21, 1275–1346. https://doi.org/10.1016/S0277-3791(01)00075-0.

EU WFD, 2000. Directive 2000/60/EC of the European parliament and of the council of establishing a framework for Community action in the field of water policy. Off. J. Eur. Communities L 327 (1), 1–72.

Even, S., Billen, G., Bacq, N., Théry, S., Ruelland, D., Garnier, J., Cugier, P., Poulin, M., Blanc, S., Lamy, F., Paffoni, C.,: New tools for modelling water quality of hydrosystems: An application in the Seine River basin in the frame of the Water Framework Directive, Sci Total Environ, 375, 1–3, https://doi.org/10.1016/j.scitotenv.2006.12.019., 2007.

Fleckenstein, J.H., Krause, S., Hannah, D.M., Boano, F., 2010. Groundwater-surface water interactions: new methods and models to improve understanding of processes and dynamics. Adv. Water Resour. 33, 1291–1295. https://doi.org/10.1016/j.advwatres.2010.09.011.

Frei, S., Gilfedder, B.S., 2015. FINIFLUX: An implicit finite element model for quantification of groundwater fluxes and hyporheic exchange in streams and rivers using radon. Water Resour. Res. 51, 6776–6786. https://doi.org/10.1002/2015WR017212.

Frei, S., Durejka, S., Le Lay, H., Thomas, Z., Gilfedder, B.S., 2019. Quantification of hyporheic nitrate removal at the reach scale: exposure times versus residence times. Water Resour. Res 55, 9808–9825. https://doi.org/10.1029/2019WR025540.

Gardner, W.P., Harrington, G.A., Solomon, D.K., Cook, P.G., 2011. Using terrigenic 4He to identify and quantify regional groundwater discharge to streams. Water Resour. Res 47, W06523. https://doi.org/10.1029/2010WR010276.

Gilliam, J., Baker, J., Reddy, K., 1999. Water Quality Effects of Drainage in Humid Regions. In: Skaggs, R., Schilfgaarde, J. (Eds.), In Agricultural Drainage. https://doi.org/10.2134/agronmonogr38.c24.

Gleeson, T., Wada, Y., Bierkens, M.F.P., van Beek, L.P.H., 2012. Water balance of global aquifers revealed by groundwater footprint. Nature 488, 197–200. https://doi.org/10.1038/nature11295.

Gu, C., Anderson Jr., W., Maggi, F., 2012. Riparian biogeochemical hot moments induced by stream fluctuations. Water Resour. Res 48, W09546. https://doi.org/10.1029/2011WR011720.

Hardenbicker, P., Weitere, M., Ritz, S., Schöll, F., Fischer, H., 2016. Longitudinal plankton dynamics in the rivers rhine and elbe. River Res Applic 32, 1264–1278. https://doi.org/10.1002/rra.2977.

Hassan, S.T., Lubczynski, M.W., Niswonger, R.G., Su, Z., 2014. Surface–groundwater interactions in hard rocks in Sardon Catchment of western Spain: an integrated modeling approach. In: J Hydrology, 517, pp. 390–410. https://doi.org/10.1016/j.jhydrol.2014.05.026.

HELCOM: HELCOM Copenhagen Ministerial Declaration, Baltic Sea Action Plan – 2021 update, https://helcom.fi/media/publications/Baltic-Sea-Action-Plan-2021-update.pdf, last access: 23. November 2021, 2021.

Hillel, N., Wine, M., Laronne, J.B., Licha, T., Be'eri-Shlevin, Y., Siebert, C., 2019. Identifying spatiotemporal variations in groundwater-surface water interactions using shallow pore water chemistry in the Lower Jordan River. Adv. Water Resour. 131, 103388 https://doi.org/10.1016/j.advwatres.2019.103388.

Howarth, R.W., Marino, R., 2006. Nitrogen as the limiting nutrient for eutrophication in coastal marine ecosystems: evolving views over three decades. Limnol. Oceano 51, 364–376. https://doi.org/10.4319/lo.2006.51.1_part_2.0364.

Hutchins, M.G., Abesser, C., Prudhomme, C., Elliott, J.A., Bloomfield, J.P., Mansour, M.M., Hitt, O.E., 2018. Combined impacts of future land-use and climate stressors on water resources and quality in groundwater and surface waterbodies of the upper Thames river basin, UK. Sci. Total Environ. 631–632, 962–986. https://doi.org/10.1016/j.scitotenv.2018.03.052.

Ibáñez, C., Peñuelas, J., 2019. Changing nutrients, changing rivers. Science 365, 637–638. https://doi.org/10.1126/science.aay2723.

IKSE: The Elbe and its catchment area. A geographical-hydrological and water management overview, 262 p., Magdeburg, 2005.

IPCC: Global Warming of 1.5°C - an IPCC Special Report: https://www.ipcc.ch/sr15/, last access: 23. November 2021, Masson-Delmotte, V., P. Zhai, H.-O. Pörtner, D. Roberts, J. Skea, P.R. Shukla,A. Pirani, W. Moufouma-Okia, C. Péan, R. Pidcock, S. Connors, J.B.R. Matthews, Y. Chen, X. Zhou, M.I. Gomis, E. Lonnoy, T. Maycock,M. Tignor, T. Waterfield, in press, 2018.

Jarvis, P., Rey, A., Petsikos, C., Wingate, L., Rayment, M., Pereira, J., Banza, J., David, J., Miglietta, F., Borghetti, M., Manca, G., Valentini, R., 2007. Drying and wetting of Mediterranean soils stimulates decomposition and carbon dioxide emission: the "Birch effect". Tree Physiol. 27, 929–940. https://doi.org/10.1093/treephys/27.7.929.

Kalbus, E., Reinstorf, F., Schirmer, M., 2006. Measuring methods for groundwater–surface water interactions: a review. Hydrol. Earth Syst. Sc. 10, 873–887. https://doi.org/10.5194/hess-10-873-2006.

Kalugin, A.S., 2019. The impact of climate change on surface, subsurface, and groundwater flow: a case study of the Oka River (European Russia). Water Resour. 46, S31–S39. https://doi.org/10.1134/S0097807819080104.

Kamjunke, N., Rode, M., Baborowski, M., Kunz, J.V., Zehner, J., Borchardt, D., Weitere, M., 2021. High irradiation and low discharge promote the dominant role of phytoplankton in riverine nutrient dynamics. Limnol. Oceano 66, 2648–2660. https://doi.org/10.1002/lno.11778.

Kamjunke, N., Beckers, L., Herzsprung, P., von Tümpling, W., Lechtenfeld, O., Tittel, J., Risse-Buhl, U., Rode, M., Wachholz, A., Kallies, R., Schulze, T., Krauss, M., Brack, W., Comero, S., Gawlik, B.M., Skejo, H., Tavazzi, S., Mariani, G., Borchardt, D., Weitere, M., 2022. Lagrangian profiles of riverine autotrophy, organic matter transformation, and micropollutants at extreme drought. Sci. Total Environ. 828, 154243 https://doi.org/10.1016/j.scitotenv.2022.154243.

Kerr, J.G., Burford, M.A., Olley, J., Udy, J., 2010. The effects of drying on phosphorus sorption and speciation in subtropical river sediments. Mar. Freshw. Res 61, 928–935. https://doi.org/10.1071/MF09124.

King, K.W., Fausey, N.R., Williams, M.R., 2014. Effect of subsurface drainage on streamflow in an agricultural headwater watershed. J. Hydrol. 519, 438–445. https://doi.org/10.1016/j.jhydrol.2014.07.035.

Lalot, E., Curie, F., Wawrzyniak, V., Baratelli, F., Schomburgk, S., Flipo, N., Piegay, H., Moatar, F., 2015. Quantification of the contribution of the Beauce groundwater aquifer to the discharge of the Loire River using thermal infrared satellite imaging. Hydrol. Earth Syst. Sci. 19, 4479–4492. https://doi.org/10.5194/hess-19-4479-2015.

Larned, S.T., Hicks, D.M., Schmidt, J., Davey, A.J.H., Dey, K., Scarsbrook, M., Arscott, D.B., Woods, R.A., 2008. The Selwyn River of New Zealand: a benchmark system for alluvial plain rivers. River Res Appl. 24, 1–21. https://doi.org/10.1002/rra.1054.

Larned, S.T., Unwin, M.J., Boustead, N.C., 2015. Ecological dynamics in the riverine aquifers of a gaining and losing river, Freshwater. Sci 34, 245–262. https://doi.org/10.1086/678350.

Larroudé, S., Massei, N., Reyes-Marchant, P., Delattre, C., Humbert, J., 2013. Dramatic changes in a phytoplankton community in response to local and global pressures: a 24-year survey of the river Loire (France). Glob. Change Biol. 19, 1620–1631. https://doi.org/10.1111/gcb.12139.

Lasagna, M., De, Luca, Franchino, D., 2016. E.: Nitrate contamination of groundwater in the western Po Plain (Italy): the effects of groundwater and surface water interactions. Environ. Earth Sci. 75, 240. https://doi.org/10.1007/s12665-015-5039-6.

Lewandowski, J., Meinikmann, K., Nützmann, G., Rosenberry, D.O., 2015. Groundwater – the disregarded component in lake water and nutrient budgets. Part 2: Eff. Groundw. Nutr., Hydrol. Process 29, 2922–2955. https://doi.org/10.1002/hyp.10384.

LfULG Saxony: Drainage systems in Saxony, Importance of agricultural drainage systems for the water and matter budget, Issue 28/2013, State Office for the Environment, Agriculture and Geology Saxony, 2013.

LfULG Saxony: Data portal iDA (interdisciplinary data and evaluations) of the State Office for the Environment, Agriculture and Geology Saxony, https://www.umwelt.sachsen.de/umwelt/46037.htm, last access: 15. April 2021, 2020.

Malard, F., Mangin, A., Uehlinger, U., Ward, J.V., 2001. Thermal heterogeneity in the hyporheic zone of a glacial floodplain. Can. J. Fish. Aquat. Sci. 58, 1319–1335. https://doi.org/10.1139/cjfas58-7-1319.

Mallast, U., Staniek, M., Koschorreck, M., 2020. Spatial upscaling of CO_2 emissions from exposed river sediments of the Elbe River during an extreme drought. Ecohydrology 13, e2216. https://doi.org/10.1002/eco.2216.

Mallin, M.A., Johnson, V.L., Ensign, S.H., MacPherson, T.A., 2006. Factors contributing to hypoxia in rivers, lakes, and streams. Limnol. Oceano 51, 690–701. https://doi.org/10.4319/lo.2006.51.1_part_2.0690.

McCallum, J.L., Cook, P.G., Brunner, P., Berhane, D., 2010. Solute dynamics during bank storage flows and implications for chemical base flow separation. Water Resour. Res 46, W07541. https://doi.org/10.1029/2009WR008539.

McCallum, J.L., Cook, P.G., Berhane, D., Rumpf, C., McMahon, G., 2012. Quantifying groundwater flows to streams using differential flow gaugings and water chemistry. J. Hydrol. 416–417, 118–132. https://doi.org/10.1016/j.jhydrol.2011.11.040.

Merz, R., Blöschl, G., 2003. A process typology of regional floods. Water Resour. Res. 39 (12), 1340. https://doi.org/10.1029/2002WR001952.

Moore, W., 1997. High fluxes of radium and barium from the mouth of the Ganges-Brahmaputra River during low river discharge suggest a large groundwater source. Earth Planet Sc. Lett. 150, 141–150. https://doi.org/10.1016/S0012-821X(97)00083-6.

Mostert, E., 2008. International co-operation on Rhine water quality 1945–2008: an example to follow? Phys. Chem. Earth, Parts A/B/C. 34, 142–149. https://doi.org/10.1016/j.pce.2008.06.007.

Neal, C., Williams, R.J., Neal, M., Bhardwaj, L.C., Wickham, H., Harrow, M., Hill, L.K., 2000. The water quality of the River Thames at a rural site downstream of Oxford. Sci. Total Environ. 251–252, 441–457. https://doi.org/10.1016/S0048-9697(00)00398-3.

Oehler, T., Eiche, E., Putra, D., Adyasari, D., Hennig, E., Mallast, U., Moosdorf, N., 2018. Seasonal variability of land-ocean groundwater nutrient fluxes from a tropical karstic region (southern Java, Indonesia). J. Hydrol. 565, 662–671. https://doi.org/10.1016/j.jhydrol.2018.08.077.

Oppermann, R., Schuhmacher, F., Kirchesch, V., 2015. HYDRAX: A 1-D hydrodynamic model, 10.5675/HYDRAX,Coblenz Math. Model data Interfaces, BfG Rep. 1872, 54, 10.5675/HYDRAX,Coblenz.

Ortega, L., Manzano, M., Custodio, E., Hornero, J., Rodríguez-Arévalo, J., 2015. Using 222Rn to identify and quantify groundwater inflows to the Mundo River (SE Spain). Chem. Geol. 395, 67–79. https://doi.org/10.1016/j.chemgeo.2014.12.002.

OSPAR: OSPAR Commission - Convention for the Protection of the Marine Environment of the North-East Atlantic, https://www.ospar.org/work-areas/hasec/other/strategies, last access: 23. November 2021, 2021.

Panepinto, D., Marchese, F., Genon, G., 2015. Evaluation of Po River water quality in Torino (Italy): effects of diffuse and local point loads. Urban Water J. 13 (6), 583–599. https://doi.org/10.1080/1573062X.2015.1011669.

Parkhurst, D.L., Appelo, C.A.J., 2013. Description of input and examples for PHREEQC version 3—A computer program for speciation, batch-reaction, one-dimensional transport, and inverse geochemical calculations. U. S. Geol. Surv. Tech. Methods, Book 6, chap A43, 497.

Pavelis, G.A., 1987. Farm Drainage in the United States. History, Status, and Prospects, Economic Research Service. U.S. Department of Agriculture, Miscellaneous Publication Number 1455, Washington, D.C.

Prudhomme, C., Giuntoli, I., Robinson, E.L., Clark, D.B., Arnell, N.W., Dankers, R., Fekete, B.M., Franssen, W., Gerten, D., Gosling, S.N., Hagemann, S., Hannah, D.M., Kim, H., Masaki, Y., Satoh, Y., Stacke, T., Wada, Y., Wisser, D., 2013. Hydrological droughts in the 21st century, hotspots and uncertainties from a global multimodel ensemble experiment. Proc. Natl. Acad. Sci. USA 111, 3262–3267. https://doi.org/10.1073/pnas.1222473110.

Puckett, L.J., Zamora, C., Essaid, H., Wilson, J.T., Johnson, H.M., Brayton, M.J., Vogel, J.R., 2008. Transport and fate of nitrate at the ground-water/surface-water interface. J. Environ. Qual. 37, 1034–1050. https://doi.org/10.2134/jeq2006.0550.

Rhodes, K.A., Proffitt, T., Rowley, T., Knappett, P.S.K., Montiel, D., Dimova, N., Tebo, D., Miller, G.R., 2017. Importance of bank storage in supplying baseflow to rivers flowing through compartmentalized, alluvial aquifers. Water Resour. Res 53 (10), 539–10.557. https://doi.org/10.1002/2017WR021619.

Richter, B.D., Davis, M.M., Apse, C., Konrad, C., PRESUMPTIVE, A., 2012. Standard for environmental flow protection. River Res. Applic. 28, 1312–1321. https://doi.org/10.1002/rra.1511.

Rode, M., Suhr, U., 2007. Uncertainties in selected river water quality data. Hydrol., Earth Syst. Sci. 11, 863–874. https://doi.org/10.5194/hess-11-863-2007.

Rosenberry, D.O., LaBaugh, J.W., 2008. Field techniques for estimating water fluxes between surface water and groundwater (Reston, Va). U. S. Geol. Surv. Tech. Methods 4–D2 (128). https://doi.org/10.3133/tm4D2.

Santos, I.R., Chen, X., Lecher, A.L., et al., 2021. Submarine groundwater discharge impacts on coastal nutrient biogeochemistry. Nat. Rev. Earth Environ. 2, 307–323. https://doi.org/10.1038/s43017-021-00152-0.

L.H.W. Saxony-Anhalt: Data portal DHI WASY of the Saxony-Anhalt Regional Hydrological Service in the State Office for Flood Protection and Water Management Saxony-Anhalt, https://gld-sa.dhi-wasy.de/GLD-Portal/, last access: 11. May 2021, 2020.

L.L.G. Saxony-Anhalt: Extent of melioration systems in present-day Saxony-Anhalt, https://llg.sachsen-anhalt.de/fileadmin/Bibliothek/Politik_und_Verwaltung/MLU/LLFG/Dokumente/04_themen/agraroekologie/15_umfang-von-meliorationsanlagen_link1.pdf, last access 26. October 2021.

Schletterer, M., Shaporenko, S.I., Kuzovlev, V.V., Minin, A.E., Van Geest, G.J., Middelkoop, H., Górski, K., 2019. The Volga: management issues in the largest river basin in Europe. River Res Applic 35, 510–519. https://doi.org/10.1002/rra.3268.

Schmidt, A., Stringer, C.E., Haferkorn, U., Schubert, M., 2009. Quantification of groundwater discharge into lakes using radon-222 as naturally occurring tracer. Environ. Geol. 56, 855–863. https://doi.org/10.1007/s00254-008-1186-3.

Schmidt, A., Gibson, J.J., Santos, I.R., Schubert, M., Tattrie, K., Weiß, H., 2010. The relevance of groundwater discharge to the overall water budget of two typical Boreal lakes in Alberta/Canada estimated from a radon mass balance. Hydrol. Earth Syst. Sc. 14, 79–89. https://doi.org/10.5194/hessd-6-4989-2009.

Schmidt, A., Frank, G., Stichler, W., Duester, L., Steinkopff, T., Stumpp, C., 2020. Overview of tritium records from precipitation and surface waters in Germany. Hydrol. Process. 34, 1489–1493. https://doi.org/10.1002/hyp.13691.

Schubert, M., Siebert, C., Knoeller, K., Roediger, T., Schmidt, A., Gilfedder, B., 2020. Investigating groundwater discharge into a major river under low flow conditions based on a radon mass balance supported by tritium data. Water 12, 2838. https://doi.org/10.3390/w12102838.

Sharpley, A.N., Chapra, S.C., Wedepohl, R., Sims, J.T., Daniel, T.C., Reddy, K.R., 1994. Managing agricultural phosphorus for protection of surface waters: issues and options. J. Environ. Qual. 23, 437–451. https://doi.org/10.2134/jeq1994.00472425002300030006x.

Skaggs, R.W., Brevé, M.A., Gilliam, J.W., 1994. Hydrologic and water quality impacts of agricultural drainage*. Crit. Rev. Environ. Sci. Technol. 24, 1–32. https://doi.org/10.1080/10643389409388459.

Smith, D.R., King, K.W., Johnson, L., Francesconi, W., Richards, P., Baker, D., Sharpley, A.N., 2015. Surface runoff and tile drainage transport of phosphorus in the midwestern United States. J. Environ. Qual. 44, 495–502. https://doi.org/10.2134/jeq2014.04.0176.

Tong, Y., Zhao, Y., Zhen, G., Chi, J., Liu, X., Lu, Y., Wang, X., Yao, R., Chen, J., Zhang, W., 2015. Nutrient loads flowing into coastal waters from the main rivers of China (2006–2012). Sci. Rep. 5, 16678. https://doi.org/10.1038/srep16678.

UBA: Federal Environmental Agency, Nitrogen and phosphorus loads from point and diffuse sources to surface waters in Germany, https://www.umweltbundesamt.de/sites/default/files/medien/384/bilder/dateien/2_abb_n-p-eintraege_2020–09-17.pdf, last access: 02. November.2021, 2020.

Unland, N.P., Cartwright, I., Andersen, M.S., Rau, G.C., Reed, J., Gilfedder, B.S., Atkinson, A.P., Hofmann, H., 2013. Investigating the spatio-temporal variability in groundwater and surface water interactions: a multi-technique approach. Hydrol. Earth Syst. Sci. 17, 3437–3453. https://doi.org/10.5194/hess-17-3437-2013.

Vincent, C., 2005. Hydrogeology of the Upper Selwyn Catchment, M.Sc. in. Engineering Geology. University of Canterbury, Christchurch, New Zealand.

Vogt, T., Schneider, P., Hahn-Woernle, L., Cirpka, O.A., 2010. Estimation of seepage rates in a losing stream by means of fiber-optic high-resolution vertical temperature profiling. J. Hydrol. 380, 154–164. https://doi.org/10.1016/j.jhydrol.2009.10.033.

Wang, B., Jin, M., Nimmo, J.R., Yang, L., Wang, W., 2008. Estimating groundwater recharge in Hebei Plain, China under varying land use practices using tritium and bromide tracers. J. Hydrol. 356, 209–222. https://doi.org/10.1016/j.jhydrol.2008.04.011.

Wilmsen, M., Niebuhr, B., 2014. Cretaceous in Saxony, Geologica Saxonica. J. Cent. Eur. Geol., 60, 3-12, Senckenberg Nat. Hist. Collect., Dresd.

Winter, T.C., Harvey, J.W., Franke, O.L., Alley, W.M., 1998. Groundwater and surface water; a single resource, US Geological Survey Circular 1139. USGS, Denver 0364–6017.

Xie, Y., Cook, P.G., Shanafield, M., Simmons, C.T., Zheng, C., 2016. Uncertainty of natural tracer methods for quantifying river–aquifer interaction in a large river. J. Hydrol. 535, 135–147. https://doi.org/10.1016/j.jhydrol.2016.01.071.

Yu, M.C.L., Cartwright, I., Braden, J.L., de Bree, S.T., 2013. Examining the spatial and temporal variation of groundwater inflows to a valley-to-floodplain river using 222Rn, geochemistry and river discharge: the Ovens River, southeast Australia. Hydrol. Earth Syst. Sci. 17, 4907–4924. https://doi.org/10.5194/hess-17-4907-2013.